

SUPPLEMENTARY INFORMATION

Functional Surface Layers in Relaxor Ferroelectrics

Nitish Kumar^{1,*}, Scarlet Kong¹, Pankaj Sharma^{1,2}, Xi Shi¹, Gaurav Vats¹, Stefano
Checchia^{3,4}, Jan Seidel^{1,2}, Mark Hoffman¹, John Daniels¹

1. School of Materials Science and Engineering, Faculty of Science, University of New South
Wales, Sydney, NSW 2052, Australia

2. ARC Centre of Excellence in Future Low-Energy Electronics Technologies (FLEET),
UNSW Sydney, Sydney NSW 2052, Australia

3. European Synchrotron Radiation Facility (ESRF), Grenoble 38000, France

4. MAX IV Laboratory, Lund University, Lund 22100, Sweden

* Corresponding author's e-mail: nitishkumar.iitk@gmail.com

Experimental Methods

Temperature-dependent permittivity measurements were performed using an LCR meter (Microtest 6376) and Probostat (NorECs Norway) at frequencies ranging from 100 Hz to 200 kHz on virgin samples, which were polished to 1 μm finish and sputtered with 60 nm thick Pt using a coater machine (Leica EM SCD050).

Scanning Electron Microscopy (SEM) (Hitachi S3400) was used to characterize the surface microstructure of sintered samples, which were polished to a 1 μm finish. Prior to SEM, thermal etching was performed on the samples at 1100 $^{\circ}\text{C}$ for 2 hours and they were sputtered with 30 nm Pt.

Energy Dispersive X-ray Spectroscopy (Bruker SOD-EDS) analysis was performed on well-polished samples with 0.04 μm surface finish. A thin carbon layer of around 20 nm was sputtered on the sample surfaces using a DCT Turbo-pumped Desktop Carbon Evaporator prior to the measurements. A voltage of 15 kV and an acquisition time of 90 s was used for all spectrum acquisitions. Each sample was analyzed by measurement at 10 randomly selected areas.

Inductively Coupled Plasma Optical Emission Spectroscopy (ICP-OES) (iCAP 6300, Thermo Fisher, USA) analysis were performed on 100 mg of fine powders for each sample, which were dried in an oven for at 100 $^{\circ}\text{C}$ for 10 hours prior to measurements.

A UV-Vis spectrophotometer (PerkinElmer Lambda 950) was used to estimate band gaps of sintered NBT-6BT, BiDef and BiXs samples. During measurements, the samples were exposed to wavelengths ranging from 200 to 1100 nm.

Photoluminescence (PL) spectroscopy was performed using a Raman Microscope (Renishaw InVia) equipped with a 325 nm excitation diode on polished ceramic surfaces. The ceramics were annealed at 500 $^{\circ}\text{C}$ for 2 hours before measurements.

Results

Table S1. Local and average compositions measured by EDS and ICP-OES of stoichiometric and non-stoichiometric NBT-6BT samples. The EDS data were obtained from measurement on 10 randomly selected areas of the samples. The mean values and standard deviations are listed. ICP-OES analysis was performed three times for each sample and the mean values are shown.[1] Both these techniques were consistent with the fact that Na:Bi ratio is highest for BiDef and lowest for BiXs.

	Bi (at %)	Na (at %)	Ba (at %)	Ti (at %)	Tested formula	Theoretical formula
EDS						
NBT-6BT	18.88 (±0.78)	19.88 (±0.61)	2.76 (±0.48)	47.77 (±0.47)	$\text{Na}_{0.42}\text{Bi}_{0.398}\text{Ba}_{0.06}\text{TiO}_x$	$\text{Na}_{0.47}\text{Bi}_{0.47}\text{Ba}_{0.06}\text{TiO}_x$
BiXs	19.59 (±0.8)	20.25 (±0.52)	2.02 (±0.30)	47.95 (±0.58)	$\text{Na}_{0.42}\text{Bi}_{0.409}\text{Ba}_{0.04}\text{TiO}_x$	$\text{Na}_{0.47}\text{Bi}_{0.479}\text{Ba}_{0.06}\text{TiO}_x$
BiDef	18.83 (±0.8)	19.74 (±0.48)	2.23 (±0.35)	46.19 (±0.48)	$\text{Na}_{0.43}\text{Bi}_{0.407}\text{Ba}_{0.06}\text{TiO}_x$	$\text{Na}_{0.47}\text{Bi}_{0.46}\text{Ba}_{0.05}\text{TiO}_x$
ICP-OES						
NBT-6BT	22.49	21.27	2.80	48.01	$\text{Na}_{0.44}\text{Bi}_{0.468}\text{Ba}_{0.06}\text{TiO}_x$	$\text{Na}_{0.47}\text{Bi}_{0.47}\text{Ba}_{0.06}\text{TiO}_x$
BiXs	22.38	20.79	2.72	46.92	$\text{Na}_{0.44}\text{Bi}_{0.476}\text{Ba}_{0.06}\text{TiO}_x$	$\text{Na}_{0.47}\text{Bi}_{0.479}\text{Ba}_{0.06}\text{TiO}_x$
BiDef	21.80	21.01	2.77	47.24	$\text{Na}_{0.44}\text{Bi}_{0.461}\text{Ba}_{0.06}\text{TiO}_x$	$\text{Na}_{0.47}\text{Bi}_{0.46}\text{Ba}_{0.05}\text{TiO}_x$

Figure S1. SEM micrograph of the stoichiometric NBT-6BT.

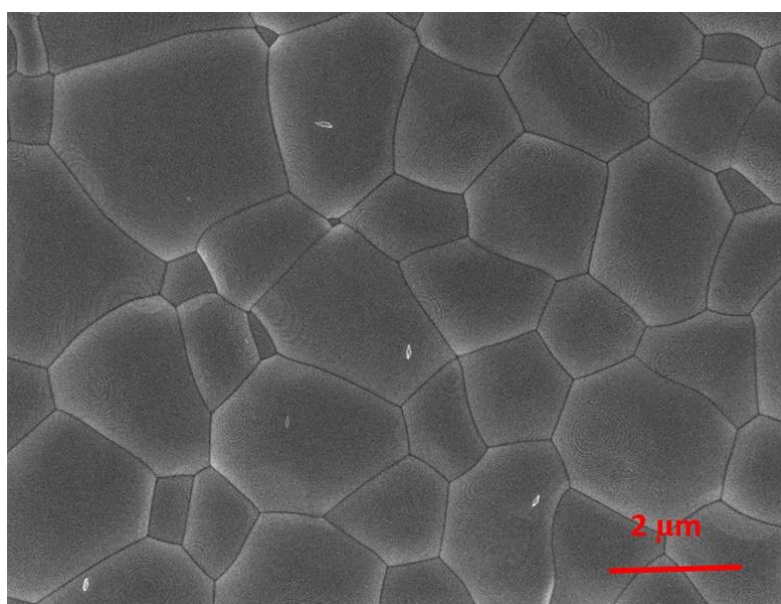


Figure S2. SEM micrographs of a BiXs (a) and BiDef (b) samples.

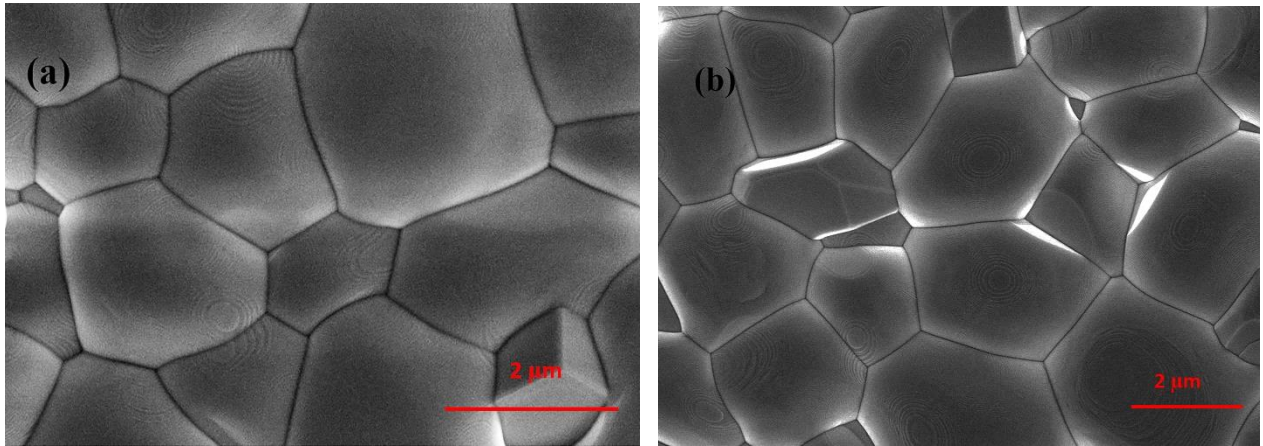


Figure S3. Permittivity, K , and dielectric loss, $\tan\delta$, as a function of temperature and frequency (f) for stoichiometric NBT-6BT sample (adapted from Ref[2]).

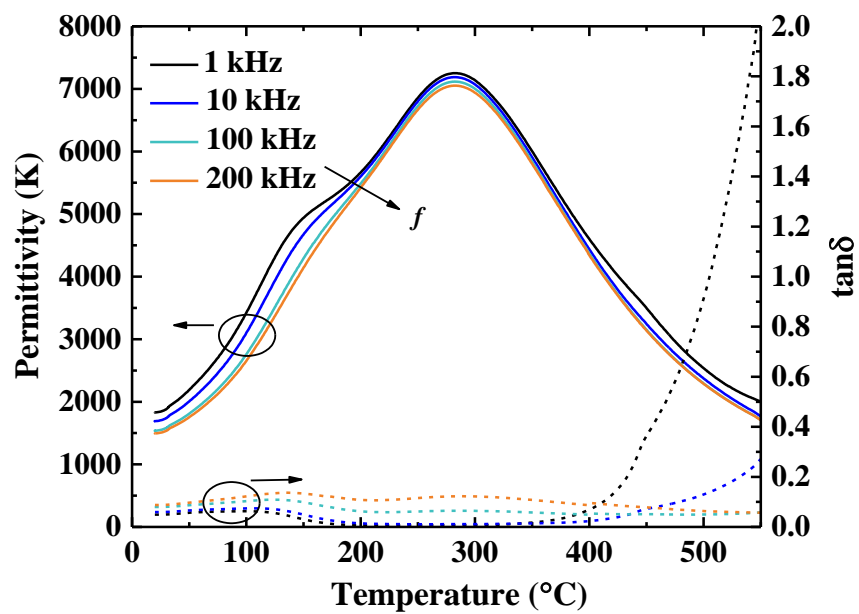


Figure S4. Permittivity, K , and dielectric loss, $\tan\delta$, as a function of temperature and frequency (f) for (a) 2% Bi-excess (BiXs) and (b) 2% Bi-deficient (BiDef) NBT-6BT (adapted from Ref[2]). The dielectric loss values become large at relatively lower temperatures for the BiDef sample as compared to the BiXs sample, which is consistent with the fact that it has higher oxygen vacancy concentration than BiXs (Equations 1-3 in the main text).

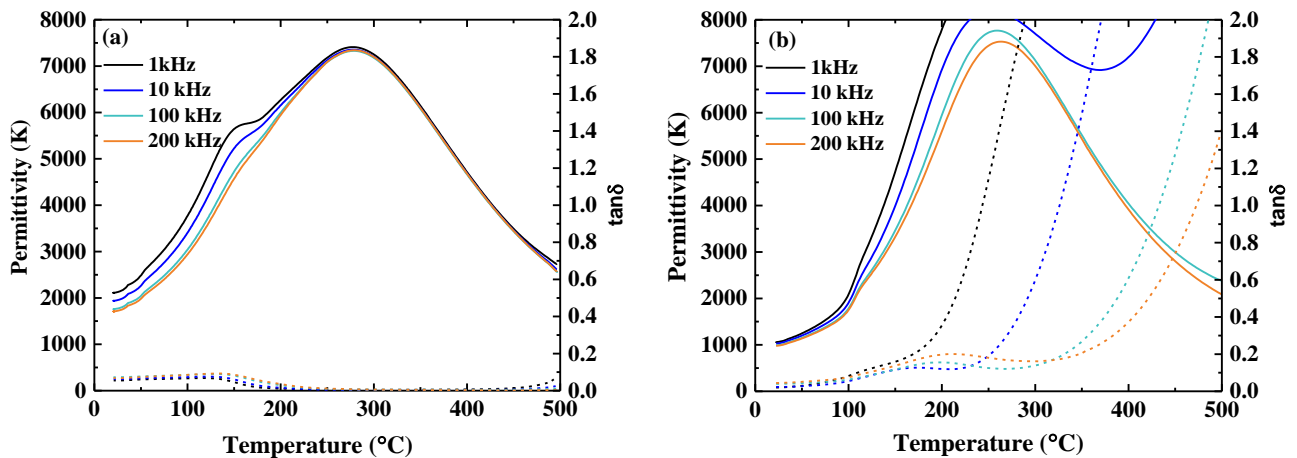


Figure S5. Kubelka-Munk plot using UV-Vis spectroscopy.[3] The raw data for reflectance was converted to $F(R)$ using the equation $F(R) = \frac{(1-R)^2}{2R}$ (where R is the reflectance). The band gap of all the three samples was estimated to be around 3.0 eV, which is consistent with the band gap for titanate perovskites.[4, 5]

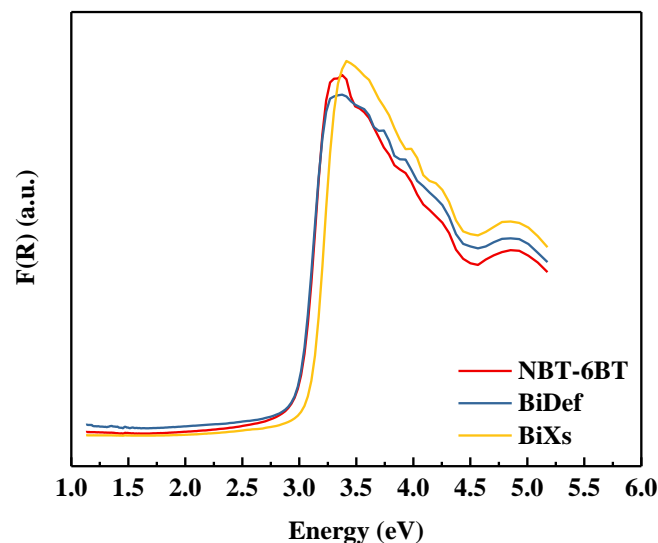


Figure S6. Photoluminescence (PL) spectra for BiDef and BiXs sample. The lowest wavelength bump was observed around 410 nm (or 3.02 eV) as indicated by an arrow, which is consistent with the bandgap measured using UV-Vis spectroscopy in Figure S5.

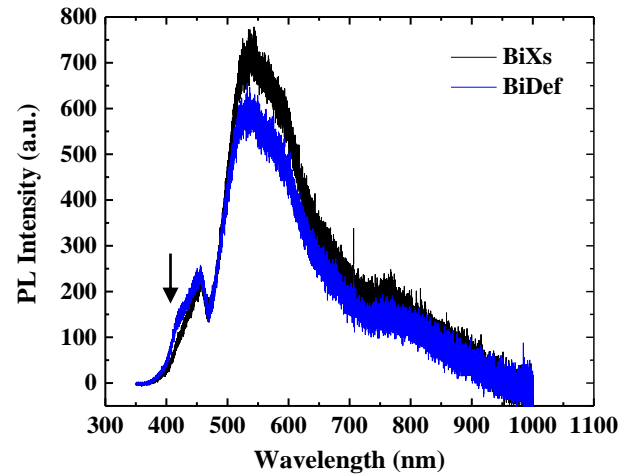
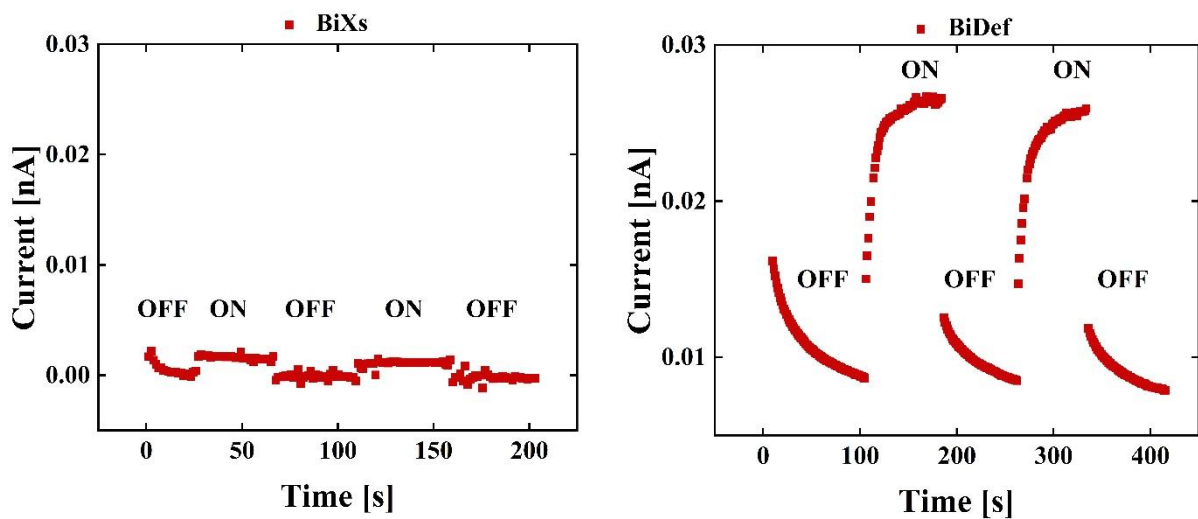


Figure S7: Change in current on light exposure. For this measurement, a voltage of 0.1 V was constantly applied to the BiXs and BiDef samples and the current was monitored as the laser was turned on and off periodically. The set-up used for this experiment was identical to the one used for Figure 4 in the main text. It can be observed that the current values increase when the laser was turned on for both BiXs and BiDef. However, the magnitude of this change was significantly larger for the BiDef sample.



References

- [1] X. Shi, N. Kumar, M. Hoffman, Electrical Fatigue Behavior of NBT-BT-xKNN Ferroelectrics: Effect of Phase Transformations and Oxygen Vacancies, *Journal of Materials Chemistry C* (Accepted) (2020) DOI: 10.1039/C9TC05665C.
- [2] X. Shi, N. Kumar, M. Hoffman, Electric field–temperature phase diagrams for $(\text{Bi}_{1/2}\text{Na}_{1/2})\text{TiO}_3\text{--BaTiO}_3\text{--}(\text{K}_{1/2}\text{Na}_{1/2})\text{NbO}_3$ relaxor ceramics, *Journal of Materials Chemistry C* 6(45) (2018) 12224-12233.
- [3] R. López, R. Gómez, Band-gap energy estimation from diffuse reflectance measurements on sol–gel and commercial TiO_2 : a comparative study, *Journal of sol-gel science and technology* 61(1) (2012) 1-7.
- [4] M. Bousquet, J.-R. Duclère, E. Orhan, A. Boule, C. Bachelet, C. Champeaux, Optical properties of an epitaxial $\text{Na}_{0.5}\text{Bi}_{0.5}\text{TiO}_3$ thin film grown by laser ablation: Experimental approach and density functional theory calculations, *Journal of Applied Physics* 107(10) (2010) 104107.
- [5] N. Kumar, D.P. Cann, Electromechanical strain and bipolar fatigue in $\text{Bi}(\text{Mg}_{1/2}\text{Ti}_{1/2})\text{O}_3\text{--}(\text{Bi}_{1/2}\text{K}_{1/2})\text{TiO}_3\text{--}(\text{Bi}_{1/2}\text{Na}_{1/2})\text{TiO}_3$ ceramics, *Journal of Applied Physics* 114(5) (2013) 054102.